Journal of Structural Geology 33 (2011) 1220–1236

Contents lists available at ScienceDirect

Journal of Structural Geology

journal homepage: www.elsevier.com/locate/jsg

Late Cretaceous extensional denudation along a marble detachment fault zone in the Kırşehir massif near Kaman, central Turkey

Côme Lefebvre [a,*], Auke Barnhoorn [a], Douwe J.J. van Hinsbergen [b,c], Nuretdin Kaymakci [d], Reinoud L.M. Vissers [a]

[a] Department of Earth Sciences, Utrecht University, 3584 CD Utrecht, The Netherlands
[b] Physics of Geological Processes, University of Oslo, Oslo, Norway
[c] Center for Advanced Study, Norwegian Academy of Science and Letters, Oslo, Norway
[d] Department of Geological Engineering, Middle East Technical University, Ankara, Turkey

ARTICLE INFO

Article history:
Received 23 February 2011
Received in revised form
13 June 2011
Accepted 14 June 2011
Available online 21 June 2011

Keywords:
Calcite mylonites
EBSD
Extensional detachment
Exhumation
Central Anatolia

ABSTRACT

In the Central Anatolian Crystalline Complex (CACC), 100 km scale metamorphic domains were exhumed in a context of north-south plate convergence during late Cretaceous to Cenozoic times. The timing, kinematics and mechanisms of exhumation have been the focus of previous studies in the southern Niğde Massif. In this study, we investigate the unexplored northern area regarding the tectonic features preserved on the edges of the Kırşehir Massif, based on detailed field-mapping in the Kaman area where high-grade metasediments, non-metamorphic ophiolites and monzonitic plutons are locally exposed together. Close to the contact with the ophiolites, west-dipping foliated marble-rich rocks display mylonites and discrete protomylonites with normal shear senses indicating a general top-to-the W–NW direction. Both of these structures have been brittlely overprinted into cataclastic corridors parallel to the main foliation. The mylonite series and superimposed brittle structures together define the Kaman fault zone. The study of the evolution of calcite deformation fabrics along an EW section supported by Electron Back Scattered Diffraction measurements (EBSD) on representative fabrics indicates that the Kaman fault zone represents an extensional detachment.

In Ömerhacılı, in the vicinity of the Baranadağ quartz-monzonite, the metamorphic sequence shows static annealing of the calcite mylonitic fabrics. This evidence suggests that intrusion took place at shallow depth (~10 km) into an already exhuming metamorphic sequence. As a consequence for the Kaman area, buried metasediments have been rapidly exhumed between 84 and 74 Ma (~1 km/Ma) where exhumation along a detachment zone, displaying a top-to-the W–NW shear motion, took place in the mid to upper crust prior to magmatic intrusion in the late Campanian. As the intrusion cut through the detachment fault, the main shearing deformation ceased. Brittle tectonics coupled with erosion likely took over during the final unroofing stages at a slower rate (<0.2 km/Ma), until the pertinent rocks reached the Earth's surface in the late Paleocene.

1. Introduction

Anatolia consists of a wide orogenic belt of Alpine age that exposes intensely deformed, metamorphosed and non-metamorphosed continental fragments, separated by oceanic sutures and/or high-pressure metamorphic belts (Şengör and Yilmaz, 1981; Okay and Tüysüz, 1999; Pourteau et al., 2010). In central Turkey, three continental domains have been recognized, i.e., (1) the Sakarya Block of the Pontides in the north that comprises a complex amalgamation of Paleozoic metamorphic terranes covered with unmetamorphosed Mesozoic succession, (2) the high-grade Kırşehir Crystallines (Bailey and McCallien, 1950) or Central Anatolian Crystalline Complex (CACC) (Göncüoğlu et al., 1991) unconformably overlain by Tertiary clastics, and (3) the non-metamorphosed Tauride thrust-belt (*sensu sitricto*) in the south. The Pontides and CACC are separated by the Izmir-Ankara-Erzincan suture zone, characterized by Permo-Triassic to Cretaceous ophiolites. The CACC and the Taurides are separated by a zone of high-pressure metamorphic rocks of late Cretaceous-Paleocene age, and the Taurides are also tectonically overlain by ophiolites (Okay et al., 1998; Candan et al., 2005). Most authors therefore

* Corresponding author.
E-mail address: come.lefebvre@gmail.com (C. Lefebvre).

0191-8141/$ – see front matter © 2011 Elsevier Ltd. All rights reserved.
doi:10.1016/j.jsg.2011.06.002

interpret a second suture zone, the Intra-Tauride suture, in between the CACC and the Taurides.

In contrast to the Pontides and Taurides, the CACC recorded mostly high-grade metamorphism, dominated by high temperature, low-pressure metasediments (Erkan, 1976; Göncüoğlu, 1977; Whitney et al., 2001) intruded by widespread plutons (Fig. 1). The age of metamorphism and magmatism is late Cretaceous (Fig. 2) (Göncüoğlu, 1986; Whitney et al., 2003; Whitney and Hamilton, 2004; Boztuğ et al., 2009b). Given the regional occurrence of remnants of ophiolites overlying the CACC, metamorphism is generally ascribed to burial of the CACC below an ocean-derived sequence.

Although the age of exhumation of the CACC as a whole is relatively well constrained by $^{40}Ar/^{39}Ar$ ages, apatite fission-track data and unconformably overlying deposits, the mechanism of exhumation is poorly understood (Seymen, 1981; Görür et al., 1998; Fayon et al., 2001; Gautier et al., 2002; Whitney et al., 2003; Boztuğ and Jonckheere, 2007; Isik et al., 2008). Exhumation of high-grade metamorphic rocks is frequently associated with regional extension. For example, the Cycladic-Menderes province, of similar dimensions as the CACC, is one of the most famous extensional metamorphic provinces in the world, and exhumation from mid-crustal depths resulted from crustal extension in metamorphic core complexes (Lister, 1984; Bozkurt and Oberhansli, 2001; Jolivet et al., 2010), after a phase of exhumation in an extrusion wedge or subduction channel (Jolivet et al., 2003; Ring et al., 2007, 2010). If regional extension played a role in the exhumation of the entire CACC, such extension has important geodynamical consequences that may even influence the interpretation of suture zone configurations prior to the late Cretaceous.

So far, only in the southernmost part of the CACC – the Niğde massif – extensional exhumation has been established with a late

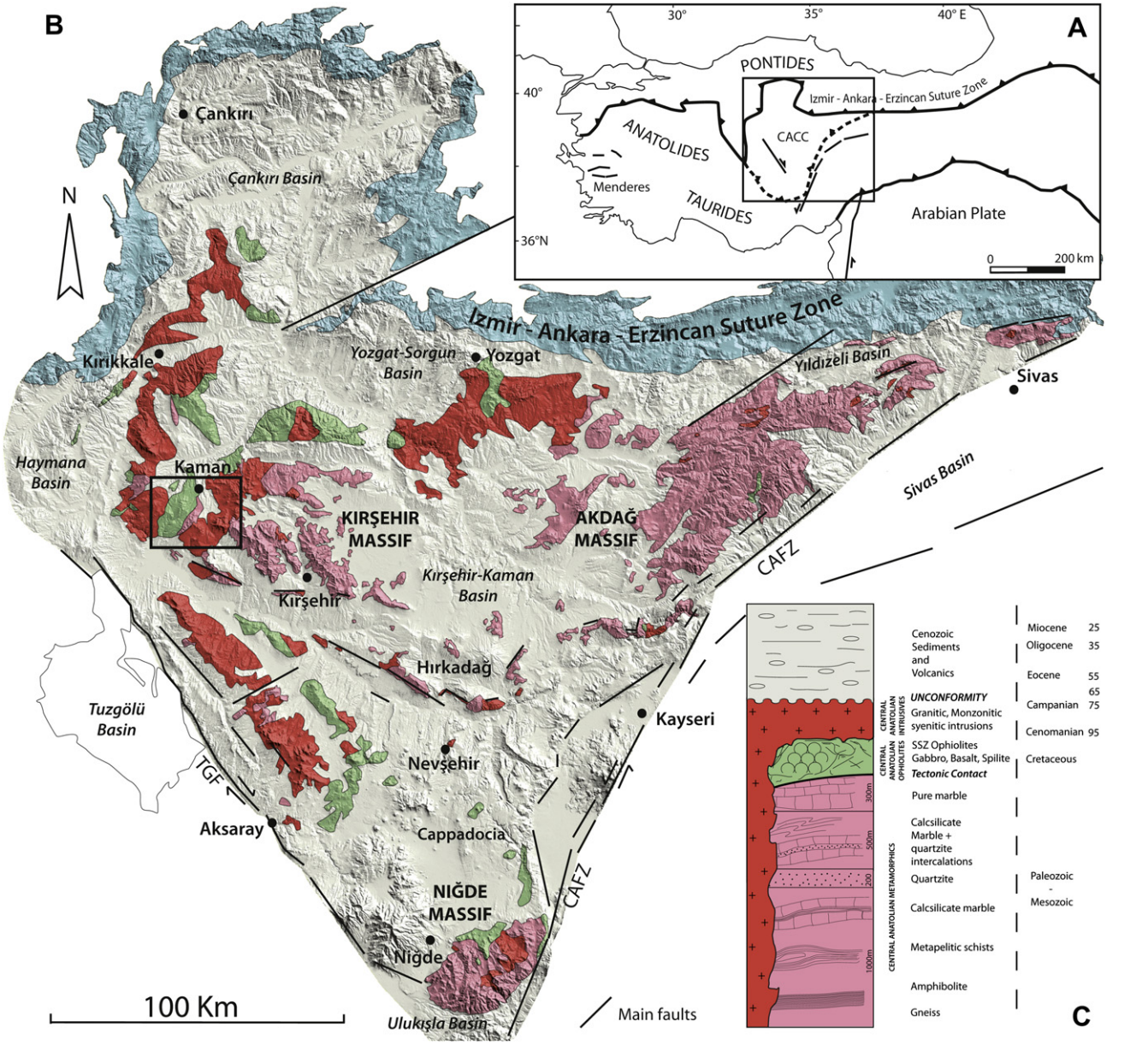

Fig. 1. (A) Location of the Menderes Massif and the Central Anatolian Crystalline Complex (CACC) in the Turkish orogenic system. (B) Simplified geological map of the CACC projected on a Digital Elevation Model. The black rectangle indicates area of study presented in Fig. 5. (C) Simplified tectono-stratigraphic column showing the relationships between the main units of the CACC (not to scale).

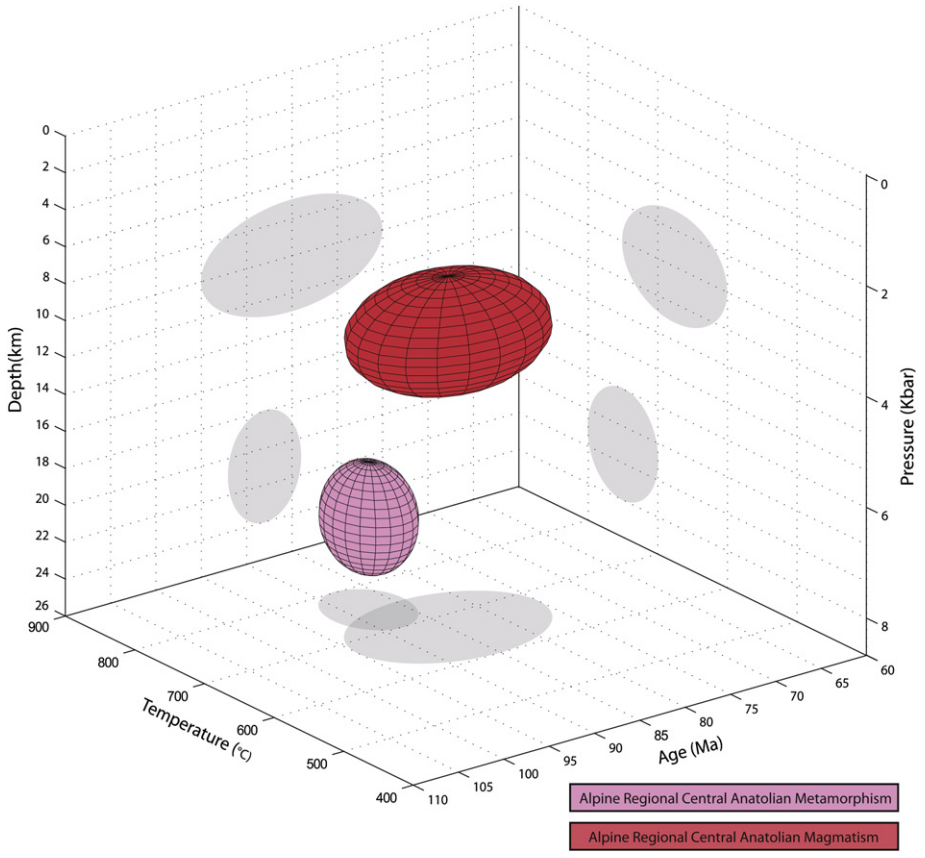

Fig. 2. Pressure-Temperature-Time diagram representing constraints on Alpine regional metamorphic and magmatic events in Central Anatolia. For pertinent references see text.

Cretaceous to Paleocene age (Gautier et al., 2002; Whitney et al., 2003; Umhoefer et al., 2007). In contrast, exhumation of the northern massifs of the CACC was postulated to relate to erosion (Fayon et al., 2001). It has, however, also been proposed that extension in the northern CACC might have been much more important that thus far considered (Dirik et al., 1999; Okay and Tüysüz, 1999; Gautier et al., 2008) and, recently, discrete extensional ductile shear zones in granitoids have been reported (Isik et al., 2008; Isik, 2009).

In this paper, we focus on the northwestern Kırşehir massif, and investigate whether tectonic extension has played a role in the exhumation of the Kırşehir metamorphics. Close to the city of Kaman, our study area provides good exposure of the contacts between the main lithological components: high-grade marbles overlain by an essentially non-metamorphic ophiolitic unit, and intruded by a monzonitic pluton (Fig. 1). The two major contacts separating them have been investigated and include (1) a tectonic contact close to Kaman separating the metamorphics from the ophiolites, and (2) the contact between the metamorphics and the monzonitic pluton in the vicinity of village of Ömerhacılı. We present field as well as optical and electron microscopy-scale, geometrical and kinematic data from the calcareous metamorphic sequence of both areas, and discuss our observations in the context of the local and regional exhumation history of the CACC.

2. Geological setting

The Central Anatolian Crystalline Complex is bounded by major tectonic features: the Izmir–Ankara–Erzincan suture in the north, the dextral Tuz Gölü fault in the west and the sinistral Central Anatolian Fault Zone in the east (Fig. 1). Inside the CACC, the main rock types encountered are: (1) Paleozoic metasediments tectonically overlain by (2) an ophiolitic sequence composed only of mafic bodies (and epi-ophiolitic cover) inferred to be of obducted origin, intruded by (3) felsic plutons and tectonically or unconformably covered by (4) non-metamorphosed volcanics and sediments of late Cretaceous to Quaternary age.

The oldest units consisting of metasediments are called Central Anatolian Metamorphics (CAM) (Göncüoğlu, 1977; Göncüoğlu et al., 1991). Despite the many metamorphic formations described in the literature, the metamorphosed stratigraphy shows a strong similarity over much of the CACC: it consists of a coherent sequence (from bottom to top) of gneiss, micaschist, quartzite, amphibolite, calcsilicate and marble. In the lowermost gneissic sequence of the Seksenuşağı Formation from the Ortakoy region, *Heliolites paekelmannophora* sp. and fragments of *Retiolites* sp. have been found pointing to a Silurian or early Devonian age (Kocak and Leake, 1994). The correlation of the marble-rich upper unit with the carbonates from the Kütahya-Bolkardağ belt in the Taurides has been used to suggest a Triassic - early Cretaceous age (Göncüoğlu et al., 1992). It follows that a Paleozoic to Mesozoic age for the central Anatolian metasediments is reasonable. This sequence of rocks underwent multiple phases of folding and pervasive ductile shearing associated with regional metamorphism during Alpine burial, intrusion and exhumation-related processes (Göncüoğlu, 1977; Seymen, 1983; Tolluoğlu and Erkan, 1989; Teklehaimanot, 1993).

The regional metamorphism ranges from greenschist to upper-amphibolite/granulite facies and is of high temperature - medium/low-pressure Barrovian type (Erkan, 1976; Seymen, 1981). Temperature and pressure at metamorphic peak conditions have been estimated at 700–800 °C for 6–8 kbar overprinted by a local

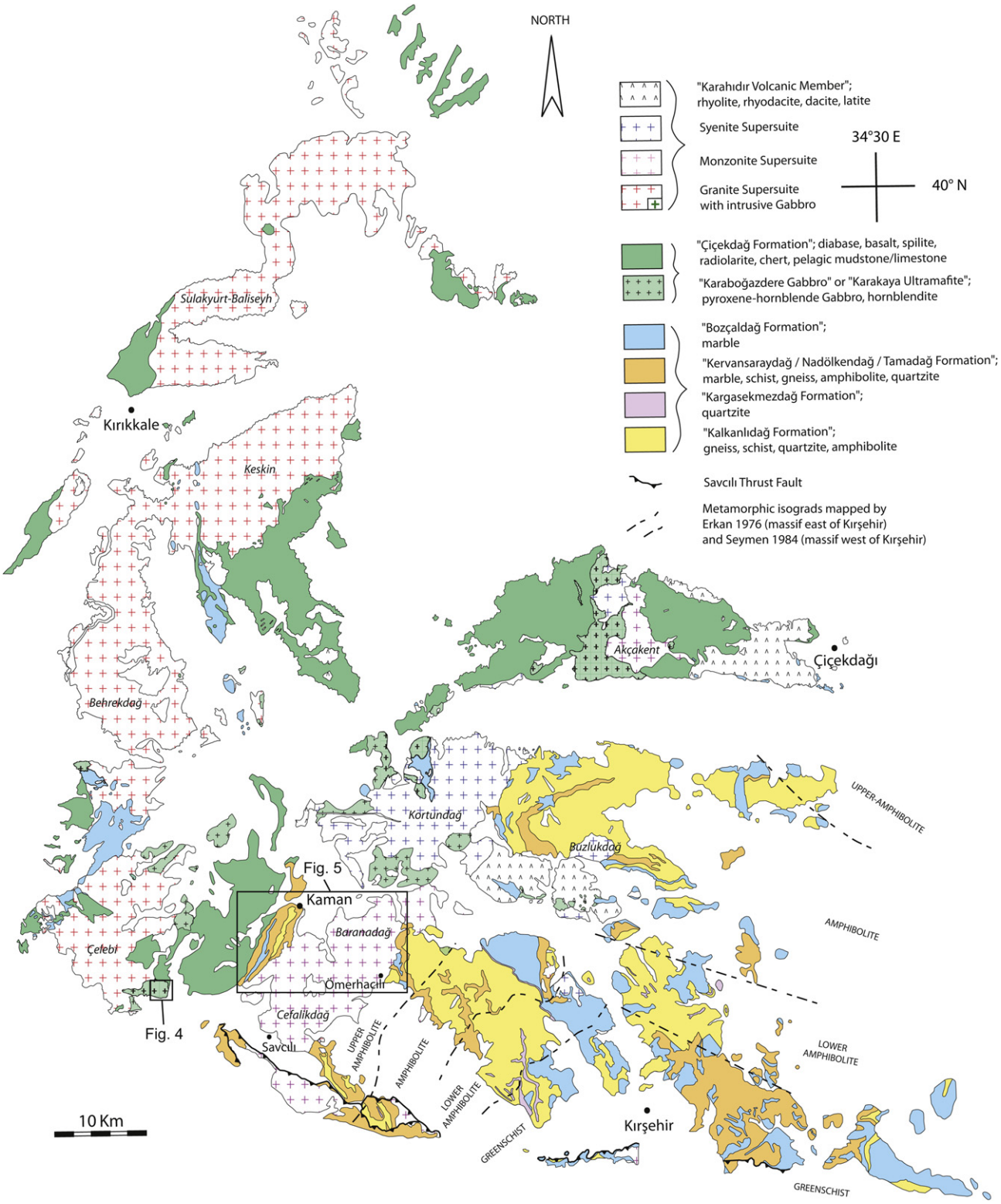

Fig. 3. Geological map of the Kırsehir massif, modified from 1:1.000.000 geological maps (MTA sheets Kırsehir-G17, G18, G19, I30, I31, I32, J30). Names of the main plutons are indicated. Also shown are published metamorphic field boundaries (Erkan, 1976 for the area east of Kırsehir city and Seymen, 1984 for the western poart of the massif). Black rectangles show the locations of Figs. 4 and 5.

re-heating at lower pressure (2–4 kbar) (Kocak and Leake, 1994; Whitney and Dilek, 1998; Whitney et al., 2001). Using U-Pb SHRIMP analysis on monazite and zircon from high-grade metapelites (Whitney et al., 2003; Whitney and Hamilton, 2004) (Fig. 2), the age of the metamorphic peak in the Kırşehir and Niğde massifs has been constrained to around 91–84 Ma.

The transition to the structurally higher unit, the Central Anatolian Ophiolites (CAO) shows evidence of fault-related features

such as tectonic breccias interpreted to be the consequence of obduction-related emplacement (Seymen, 1981; Yaliniz and Göncüoğlu, 1998). The CAO is represented by fragments of a supra-subduction zone ophiolite (SSZ) of late Cretaceous age (90–85 Ma) and partly by the upper Cretaceous accretionary complex of the "Ankara Mélange" comprising tectonized blocks of basalt, radiolarian chert, pelagic limestone and sandstone in a serpentinite matrix (Seymen, 1981; Floyd et al., 2000; Yaliniz et al., 2000).

Intruding both the CAM and CAO, the central Anatolian intrusives are widely exposed in the area (Erler and Göncüoğlu, 1996). They are generally of granitic, granodioritic, monzonitic and syenitic composition, of calcalkaline to alkaline affinity, and display characteristics of I, S and A-type granites. Their trace element geochemistry plots in the island arc, within-plate, and syn- to post-collision granitoids fields of the discrimination diagrams (Akiman et al., 1993; Aydin et al., 1998; Ilbeyli et al., 2004). Intrusion timing is constrained by Rb/Sr whole rock, U/Pb on titanite and zircon and Pb/Pb evaporation on zircon methods, and ranges from 95 to 75 Ma (Göncüoğlu, 1986; Whitney et al., 2003; Köksal et al., 2004; Boztuğ et al., 2007). Geothermobarometric calculations (Al and Ti on amphibole) indicate crystallization at ca. 600–750 °C for a pressure of ca. 2.5–4.5 kbar (Ilbeyli, 2005; Boztuğ et al., 2009a) (Fig. 2). An attempt has been made to classify the intrusives, distinguishing temporal and spatial magmatic supersuites in the area, into: (1) a Granite Supersuite associated with coeval gabbroic plutons, (2) a Monzonite Supersuite and (3) a Syenite Supersuite (Kadıoğlu et al., 2006) (Fig. 3). Cogenetic extrusives represented by rhyolite, rhyodacite, dacite, andesite and latite are also exposed in the CACC, for example in the İdişdağı area close to the Hırkadağ area (Fig. 1) (Köksal et al., 2001).

During and after exhumation of the crystalline rocks, Central Anatolian depressions were filled by volcanics and sediments. Peripheral basins floored by accretionary complexes record Late Maastrichtian to younger sedimentation (e.g. Çankırı, Haymana, Tuzgölü, Ulukışla basins) (Görür et al., 1984, 1998; Erdoğan et al., 1996, Görür et al. 1998; Çemen et al., 1999; Kaymakci et al., 2009). Intra-continental basins developed on top of the CACC since Paleocene-Eocene times (e.g. Yıldızeli, Yozgat-Sorgun, Kırşehir-Kaman basins) (Göncüoğlu, 1992; Görür et al., 1998).

Three submassifs are commonly distinguished within the CACC: the Akdağmadeni or Akdağ Massif in the north-east (Vache, 1963), the Niğde Massif in the south (Göncüoğlu, 1977) and the Kırşehir Massif in the north-west (Seymen, 1981) (Fig. 1).

The Kırşehir massif is characterized by an overall dome-shaped structure delineated by shallowly dipping foliated metamorphic rocks. The metamorphic succession is estimated to be around 2000–2500 m thick, and is made up of four units (Seymen, 1981; Tolluoğlu and Erkan, 1989) as follows. (1) The lowermost *Kalkanlıdağ Formation* is a thick unit (~1000 m) dominated by metapelitic to semi-pelitic calcareous compositions. It mainly consists of quartz-mica-schists interlayered with calcsilicate and gneissose calcschist. Few metabasites and quartzites also occur in the succession. (2) The *Kargasekmezdağ Formation* represents a homogenous quartzite layer of tens to hundreds of meters thick. (3) The *Tamadağ or Nadölkendağ Formation* (~500 m) shows the upward transition to dominantly calcareous rocks. The main lithologies are calcsilicate gneiss and impure marble, alternated with minor schist, amphibolite and quartzite bands. (4) The uppermost *Bozçaldağ Formation* consists of ~300 m of pure massive homogenous marble.

The spatial distribution of metamorphic grade throughout the Kırşehir massif has been examined using mineral isograd mapping. Three distinct metamorphic zones (corresponding to the greenschist facies and lower and upper amphibolite facies) point to an increase of the metamorphic peak temperature toward the north and north-east (Erkan, 1976). The massif situated west of Kırşehir city has been revisited, and shows an increasing grade of metamorphism from east to west, up to granulite facies conditions in the westernmost part of the section (Seymen, 1984) (Fig. 3). In this area close to the city of Kaman, thermobarometric calculations on high-grade garnet-sillimanite schist yield metamorphic equilibration around 700–750 °C at 6–7 kbar, and give an age of 84.1 ± 0.8 Ma constrained by U/Pb SHRIMP analyses on monazites (Whitney et al., 2001; Whitney and Hamilton, 2004). Moreover, a migmatite dome has been identified to the south, close to Savcılı village (Genç, 2004). During metamorphism, the metasediments underwent polyphase deformation involving three stages of superimposed folding, followed by a fracturing episode (Seymen, 1983; Tolluoğlu and Erkan, 1989).

Close to Kaman, a sharp tectonic contact separates the CAM from the CAO. The CAO is characterized by an ophiolitic sequence subdivided in the *Karaboğazdere Gabbro* or *Karakaya Ultramafite* consisting mainly of pyroxene-hornblende gabbro and hornblendite, and the *Çiçekdağ Formation* with diabase, basalt and spilite covered by epi-ophiolitic sediments such as radiolarite, chert and pelagic mudstone (Seymen, 1981, 1982). The intrusives are organized in two linear NNE-SSW trending belts. Granites and intrusive gabbros are located to the west of Kaman, and include the Sulakyurt-Baliseyh, Keskin, Behrekdağ and Çelebi granitoids. To the east, monzonitic and syenitic intrusions are represented by the Kortundağ, Hamit, Çamsarı, Bayındır and Durmuşlu plutons (Akiman et al., 1993; Otlu and Boztuğ, 1998) (Fig. 3). The Baranadağ pluton which intrudes the Kaman metamorphic sequence is made up of the Baranadağ quartz-monzonite in the north-east and the Cefalikdağ quartz-monzonite in the south-west (Seymen, 1982). The metaluminous Baranadağ quartz-monzonite is characterized by K-feldspar megacrysts and mafic enclaves, geochemically classified as H-type (hybrid) calcalkaline granitoids, but displaying a transition to alkaline chemistry, which would suggest a mature stage of post-collisional magmatism (Aydin and Önen, 1999). Crystallization ages based on U/Pb on titanite and Pb–Pb evaporation on zircon are 74.0 ± 2.8 Ma and 74.3 ± 4.5 Ma, respectively (Köksal et al., 2004; Boztuğ et al., 2009a). The cooling history of the Baranadağ quartz-monzonite is constrained by Ar/Ar on amphibole data giving plateau ages of 69–72 Ma and apatite fission-track ages around 57–60 Ma (Boztuğ et al., 2009a).

The remainder of the massif consists of depressions preserving felsic volcanics and Eocene to younger deposits resting unconformably on top of the crystalline rocks (Fig. 3). Later compression (thrusting and folding) is mostly localized in the basins situated along the edges of the massif (Tüysüz et al., 1995; Kaymakci et al., 2009). In the south, the 150 km long ESE-WNW trending Savcılı Thrust Zone is the major brittle movement zone crossing the CACC. This structure shows a NNE-vergent thrust motion between the late Eocene and late Pliocene (Fig. 3) (Seymen, 2000).

3. Characteristics of the contact between the CAM and CAO in the vicinity of Kaman

3.1. Metamorphism

An important characteristic of the contact between the Kırşehir metamorphics and the overlying CAO is the marked difference in metamorphic grade across this contact. On the western side, intrusive and extrusive mafic components of oceanic crust are represented as gabbros and basaltic lavas. The very fine-grained igneous material has a greenish matrix and contains numerous spherules filled by amorphous quartz. The green color of this unit is likely due to the presence of prehnite and/or pumpellyite as a secondary mineral assemblage. In thin section, the coarser-grained material

displays chlorite and actinolite replacing magmatic pyroxene and amphibole. Both of these secondary mineral assemblages are consistent with a low-greenschist facies overprint due to circulation of hot seawater in hydrothermal systems within the ocean floor.

To the east, the metamorphic rocks exposed immediately below the contact are clearly high-grade micaschists, calcsilicates, marbles and amphibolites. Under the optical microscope, the typical mineral assemblages in metapelites are quartz + potassic feldspar + sillimanite + garnet + biotite ± cordierite ± spinel. Metamorphosed marls contain calcite + quartz + clinopyroxene + plagioclase + garnet + sphene ± wollastonite, and metabasites consist of hornblende + plagioclase ± garnet ± clinopyroxene ± quartz. Each of the described compositions records mineral assemblages indicative of the upper amphibolites facies (confirming (Whitney et al., 2001), who estimated PT conditions around 750 °C at 7 kbar using garnet-biotite geothermobarometry).

These markedly different conditions of metamorphism, preserved on either side of the contact near Kaman, indicate that the two units underwent separate metamorphic histories involving two clearly different pathways through the crust.

3.2. Deformation

3.2.1. Hangingwall: ophiolitic sequence

To the west of Kaman, close to the Hirfanlı dam, a section through the SSZ-ophiolites exposes a layered gabbro in which clear deformational features can be observed even though the outcrop is highly altered and weathered (Fig. 4). The layering of the gabbro is compositional: lighter gabbroic layers are mainly made of pyroxene, plagioclase and amphibole, which alternate with darker layers of essentially the same mineral composition but with a much lower volume percentage of plagioclase. This primary layering has been displaced at a later stage by ~5–20 cm wide shear zones, which appear darker in the field. The offsets observed on either side of these shear zones indicate a normal shear motion. The shear planes are on average striking in a NE direction with a dip of ~40–50°. A set of two conjugate structures (one dipping toward the NW and one to the SE) can be distinguished (Fig. 4). The age of this deformation can be constrained to the time interval between the formation of this piece of oceanic crust and the exhumation of the gabbro through the brittle field. There are, unfortunately, no exposures of the ophiolitic sequence closer to the contact with the Kırşehir metamorphics that would allow a further study of its deformation history.

3.2.2. Footwall: high-grade carbonate-rich metasediments

3.2.2.1. Overall structure. In between the oceanic-derived rocks in the west and the monzonitic intrusives in the east, the Kaman metamorphics are exposed in a 2 km wide zone comprising foliated carbonate-rich metasediments. The geological map of the area (MTA sheet G17) and following publications (Seymen, 1981), show the three main metamorphic units recognized in this zone (Fig. 3). However, the presence of the *Kalkanlıdağ Formation* indicated to occur in the eastern part of the sequence has not been confirmed in the field. Instead, a major felsic dike (~250–350 m wide) is trending parallel to the main foliation. On the basis of our field observations we conclude that the Kaman metamorphics are mainly composed of pure and impure marbles intercalated with a few layers and lenses of calcsilicate, amphibolite and micaschist. The dominantly calcareous compositions indicate that the Kaman metamorphics represent the upper part of the metamorphosed lithological pile. Therefore, the detailed field map presented in Fig. 5A and b only differentiates between massive marble and bands of calcsilicates, amphibolites and calcschists.

The overall structure is characterized by a well-developed pervasive foliation parallel to compositional layering of pure carbonate layers that alternate with layers of calcsilicate, schist and amphibolite. Our measurements of the foliation planes and associated stretching lineations, compiled with previously published data (Seymen, 1983), are shown in Fig. 5A. The penetrative foliation is virtually parallel to the primary stratigraphic succession and delineates a consistent trend of about N015°E with dips commonly between 20° and 50° toward the W-NW (Fig. 5C). Note that this trend corresponds to the strike of the contact with the ophiolite. Away from the contact the foliation tends to show progressively steeper dips. Local changes in orientation are the reflection of outcrop-scale folding of the foliated banding. Optical microscopy analyses in pure and impure marbles do not show any distinct grain shape preferred orientation (GSPO), and do not preserve any stretching direction. However, foliation planes in schist and amphibolite layers, preserved stretching lineations defined by elongated mica flakes and amphiboles. In those lithologies, the measured lineations are relatively scattered, but tend to NNE-SSW trending shallow plunges (Fig. 5D). No convincing shear sense criteria have been observed in the field, due to the dominance of calcareous compositions and lack of relief exposing fresh vertical sections.

3.2.2.2. Calcite fabrics. Toward the contact, the lithology is mainly composed of pure calcite marble. In order to study the kinematics

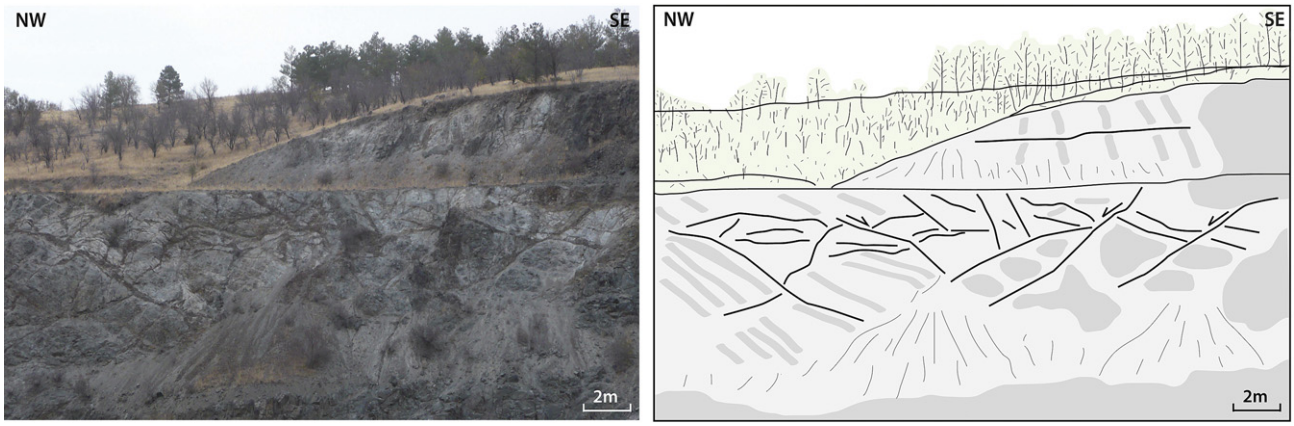

Fig. 4. Field picture and interpreted sketch from an outcrop of sheared layered gabbro belonging to the ophiolitic sequence, close to the Hirfanlı dam. In the interpretation sketch, the gabbroic body is represented in gray. Dark gray patches and layers show either fresh and/or dark plagioclase-poor gabbro. Thick black lines show the distribution of discrete shear zones cutting through the gabbroic body.

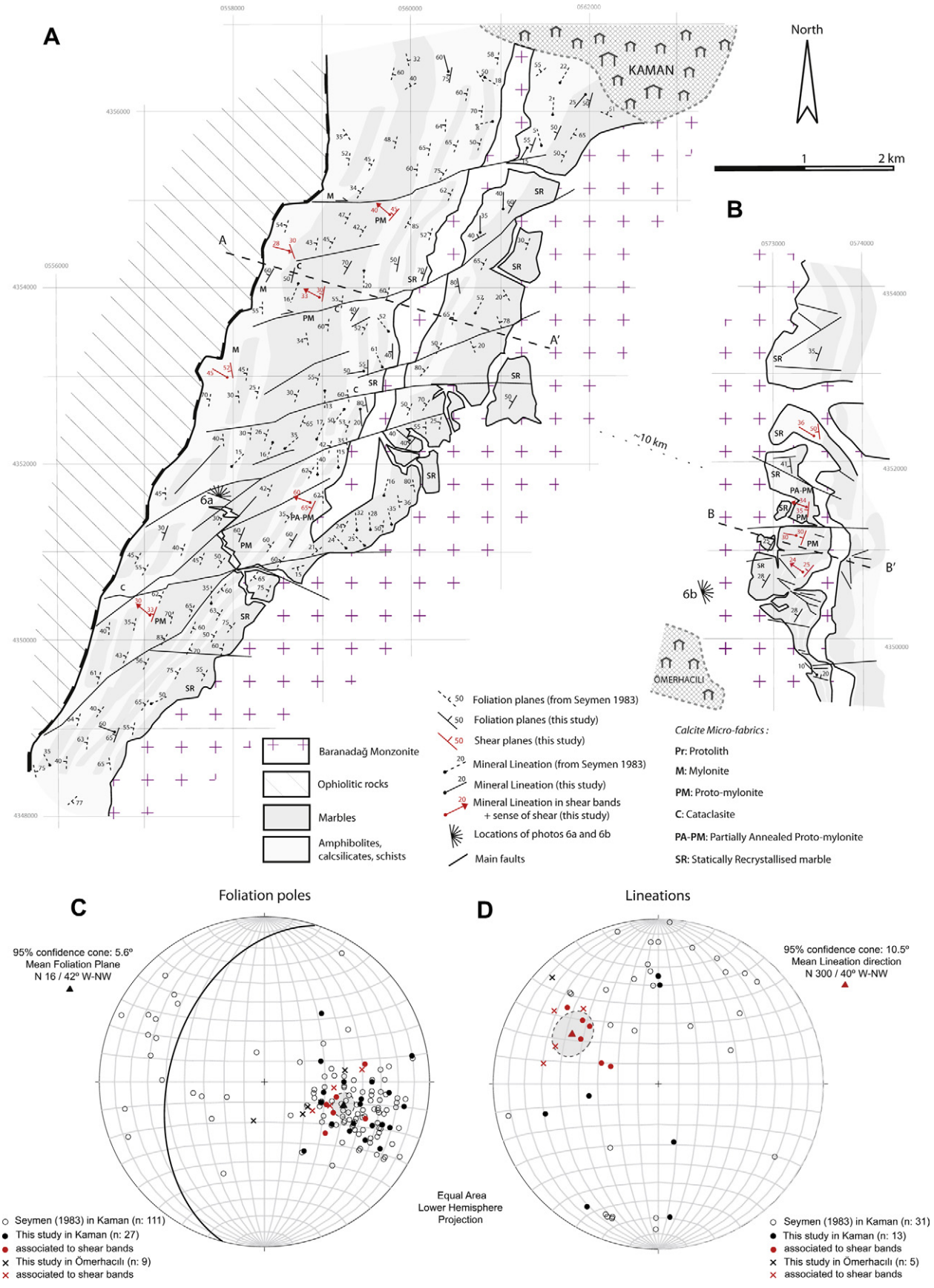

Fig. 5. (A–B) Geological and structural maps of the Kaman and Ömerhacılı areas, displaying the orientation of foliations and stretching lineations from Seymen (1983) and this study. Letter symbols indicate calcite fabrics observed in the field. Locations of panorama views and cross-sections of Fig. 6 are shown. (C) Equal area lower-hemisphere projections of foliation poles and mean foliation plane. (D) Associated stretching lineations and mean lineation direction in crosscutting shear bands.

and the deformation history related to the tectonic contact, we focused on the evolution of calcite fabrics along an east-west traverse through the carbonate-rich sequence (Fig. 6). Within the section, five marble types have been identified presumably recording different states of strain and temperature conditions during recrystallisation. On the basis of the proportion of dynamically recrystallized grains of calcite observed under optical microscope, we identified: protolith (<10%), protomylonite (10–50%), and mylonite (50–90%) types. Brecciated marbles have been defined as cataclasite, and statically recrystallized marble occurs in the vicinity of the intrusive bodies (Figs. 7 and 8). The different marble fabrics defined above show a specific spatial distribution over the area as they occur only in particular parts of the studied section as illustrated in the cross section of Fig. 6. Samples from each marble type have been studied in optical microscopy using ultra-thin sections (~10–15 μm thick), and crucial fabrics have been investigated using the Electron Back Scattered Diffraction (EBSD) technique in the scanning electron microscope. Samples for EBSD analysis were polished with colloidal silica (particle size 40 nm) for approximately 1 h and subsequently coated with a thin carbon layer. The SEM working conditions are an acceleration voltage of 25 kV, a working distance of 20 mm and a sample tilt of 70°. High-resolution EBSD maps combining both beam and stage mapping modes were performed with step sizes of 3 and 4 μm over large areas across the sample (up to 6 × 1 mm in size). Representative smaller areas were chosen from the large EBSD maps to illustrate the relationships between the different fabrics within the calcite protomylonites (Fig. 9).

3.2.2.3. Protolith (Pr). The so-called protolith consists of a coarse-grained marble (~0.5–3 mm grain size in average) mostly developed in the central part of the studied section. It represents the dominant fabric of the area and is associated with decimeter to meter wide, gray/blue and white colored banding accentuating the main foliation plane. In thin section, the grains are equigranular, euhedral to subhedral in shape, and do not show any undulose extinction. They are characterized by a high density of twin lamellae, which exhibit one to three set of twins with a vague preferred orientation. The twins are relatively thick (>>1 μm) and straight, which corresponds to type II twins following the classification of (Burkhard, 1993).

3.2.2.4. Proto-mylonite (PM). Protomylonitic fabrics are characterized by a drastic grain size reduction as compared with the protolith-type described above. In the field, protomylonites occur as localized bands (0.1–10 cm wide) crosscutting the main foliation planes (Fig. 7B), mostly within the first kilometer away from the ophiolite. The protomylonite bands are oriented parallel to the strike of the main foliation but with slightly steeper dips (Figs. 5A–C and 6A). They entirely consist of calcite grains distributed in large and elongated porphyroclasts surrounded by small equant recrystallized grains. The smaller grains are organized in bands crossing through and replacing pre-existing larger crystals,

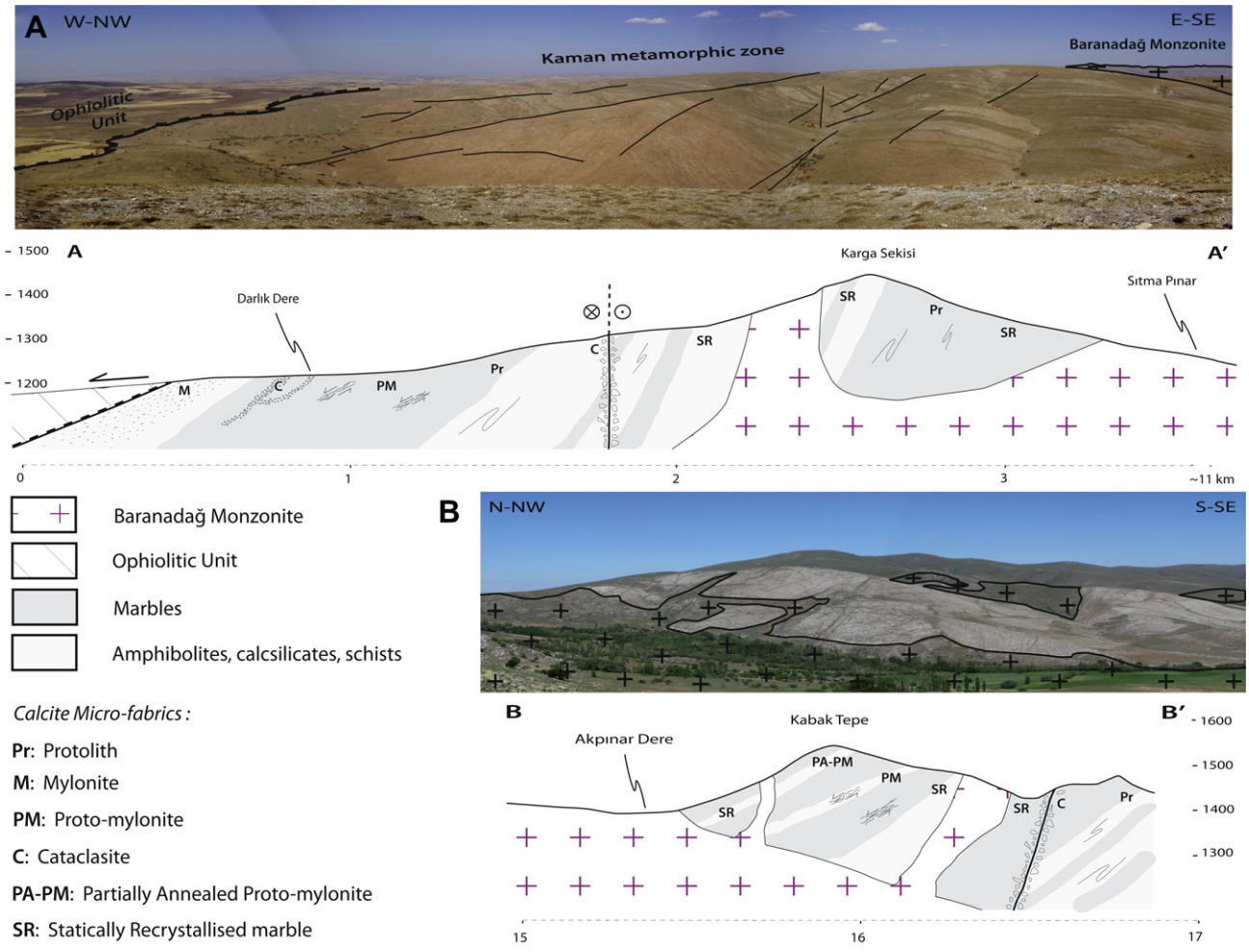

Fig. 6. Panorama views and cross-sections through Kaman (A) and Ömerhacılı (B) areas (see Fig. 5 for location). Bold letter symbols indicate the distribution of the main calcite fabrics within the calcareous metamorphic sequence.

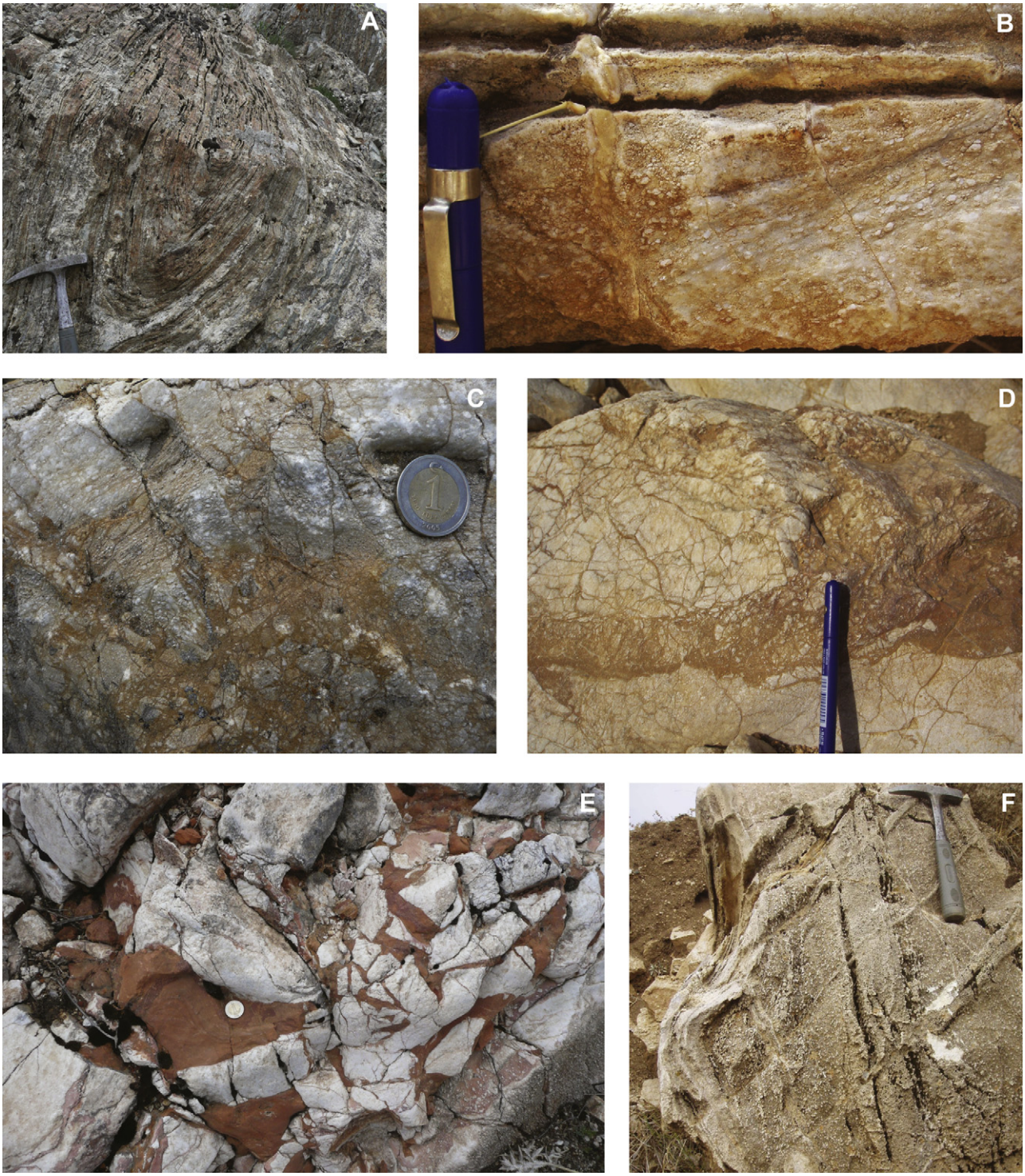

Fig. 7. Field pictures of typical marble types in Kaman area (all pictures have been taken in a north-easterly direction). A) Isoclinally folded calcsilicates. B) Crosscutting relationship between the main foliation plane and the protomylonitic shear bands. C) Protomylonitic and mylonitic marble types involved in a brecciated zone. D) Cataclastic corridors affecting protolith-type marble. E) Tectonic breccias in the vicinity of a major strike-slip fault crossing the section. F) Vertically oriented and folded very coarse-grained marble cut by oblique veins in the vicinity of Baranadağ pluton.

indicating that the change in grain size is accompanied by deformation. The bands where the deformation is concentrated are interpreted as shear bands. These bands are anastomozed around the porphyroclasts, and form conjugate zones parallel and oblique to the main shear plane (Fig. 8A). On the shear plane, the long axes of elongate porphyroclasts provide a clear marker of the stretching direction associated with the shearing. The lineations associated with those shear bands recognized over the area document a mean trend to N300°, at plunges of about 40° (Fig. 4D). In the field, the geometry of asymmetric σ-clasts has been used as a shear sense indicator consistently pointing to a top-to-WNW motion (Fig. 8A).

For microscopic observation, protomylonitic samples have been prepared perpendicular to the shear bands and parallel to the mineral lineation. The shear zone boundary is used as a reference

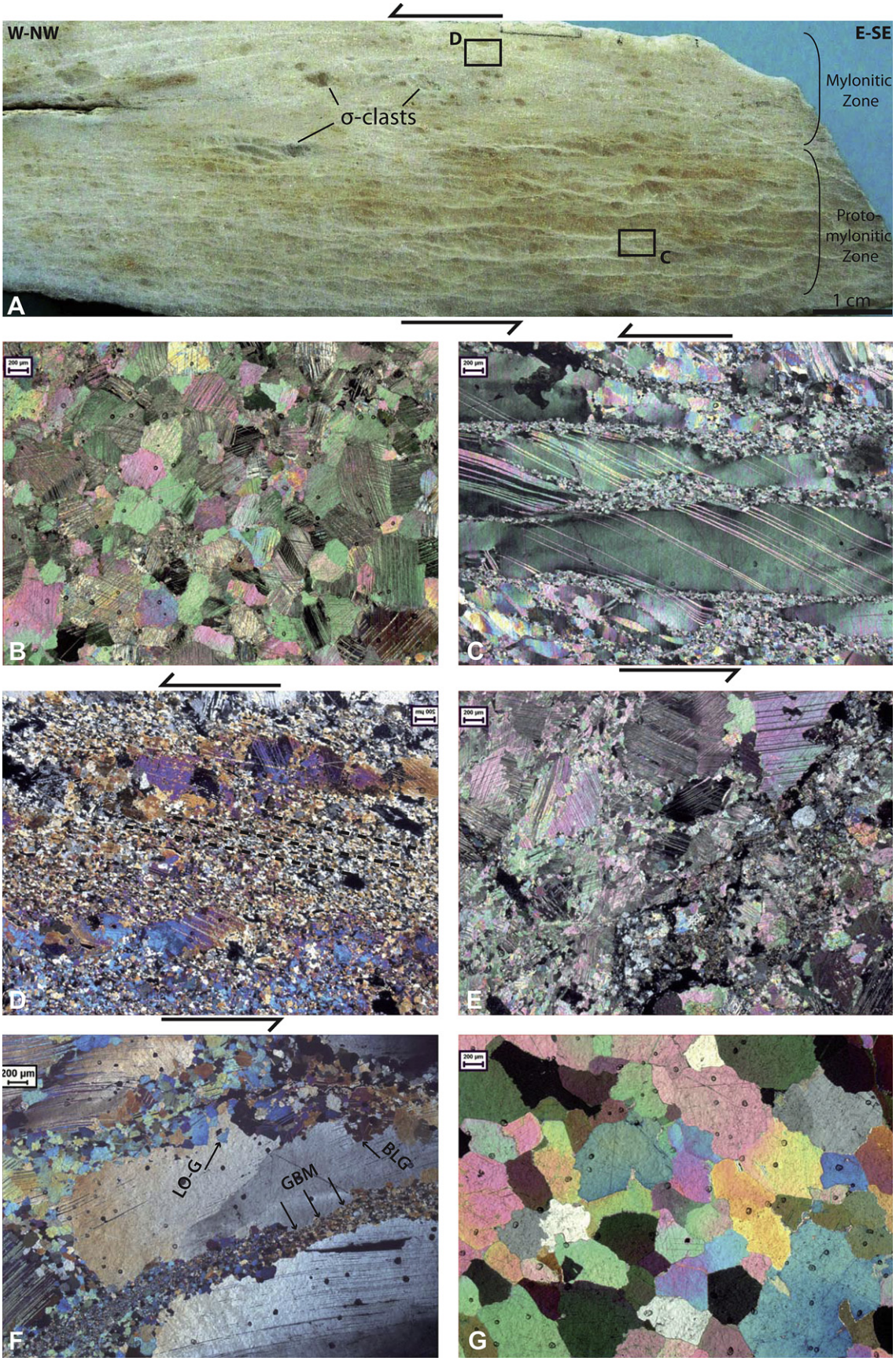

Fig. 8. A) Hand specimen of protomylonite and mylonite marble types with calcite σ-clast shear sense indicator. All calcite microstructures from (B) to (G) are shown at same magnification (scale bar = 200 µm) and oriented NW-SE (looking NE) as in Fig. 7B) Protolith type fabric, C) Protomylonite type fabric, D) Mylonite type fabric, dashed lines accentuate the grain shape preferred orientation of the dynamically recrystallized grains, E) Cataclasite type fabric, F) Partially Annealed Protomylonite type fabric, LO-G: Leftover grain, GBM: Grain boundary migration, BLG: Bulging, G) Statically recrystallised marble type fabric.

plane and shown horizontal. Numerous large calcite crystals contain a regular and dominant set of twins that are faintly bent and thus present a slightly sigmoidal shape, steeper in the centers of the grains and curving into the shear bands (Fig. 8C). Using the terminology of Burkhard (1993) these twins belong to type III indicating deformation temperatures above 200 °C. The orientation of the dominant set of twins shows a regular and systematic 30° clockwise relationship with the bands of reduced grain size. In addition to the asymmetry of the large grains, the persistent obliquity of these twins may be used to determine the shear sense (Bestmann et al., 2000), indicating a sinistral displacement with respect to the reference frame as shown in Fig. 8C. Placed back in its field context, the shearing motion indicates a normal sense where the top block is moving toward the W/NW (as also inferred in the field). The pronounced undulose extinction of many of the porphyroclasts stresses the importance of internal deformation processes such as intracrystalline slip (dislocation glide) associated with twinning.

In the shear bands, the fine-grained fabric has been characterized using electron backscatter diffraction (EBSD) measurements (Fig. 9A and B). Within those bands, we distinguished two domains with different grain size of ~17 μm and 45 μm in average (corresponding histograms in Fig. 9C).

The smaller grain domain is only composed of very fine-grained calcite grains, which are separated from each other by high angle orientation boundaries (>20°). They contain no internal structures, no twinning and show sharp extinction, as expected from subgrain rotation during dynamic recrystallization. They present an elongated shape and inclination of 10–20° clockwise to the reference plane. Pole figures of the recrystallized fine grains show typical calcite recrystallisation textures with the c-axes more or less perpendicular to the shear plane and the a-axes lying within the shear plane (c-slip on a plane) (Fig. 9D). The strong CPO patterns also point to dislocation creep activity during the formation of the protomylonites. The larger grain domain shows a similar oblique elongation pattern as the smaller grains. The larger grains show strong undulose extinction patterns, the formation of subgrains close to the grain boundaries and significant progressive rotation of the crystal lattices within the grains (misorientations of ~20° for within the 200–250 μm grains and ~10° within the 100 μm grains). CPO of the coarse grains show oblique c-axes at 45° to the shear plane which reflect the incomplete recrystallisation of the host grain within the larger grain domains that is in good agreement with microstructural observation. The presence of two domains with different grain sizes may result from the progressive localization of the deformation during exhumation.

3.2.2.5. Mylonite (M). As strain intensity increases, the marble fabrics evolve into very fine-grained ribbon mylonites as illustrated in the hand specimen shown in Fig. 8A. This microstructure is mainly present at the immediate vicinity of the contact (Fig. 6A). The mylonite type fabric consists of large clasts, which have been almost entirely dynamically recrystallized into small grains with an average grain size of 13 μm. Porphyroclast remnants are elongated parallel to the shear bands while dynamically recrystallized grains present an oblique shape preferred orientation (Fig. 8D). Small grains are relatively equigranular with no internal deformation structures. We also noted the presence of secondary phases likely due to enhanced fluid infiltration at the contact with the ophiolites.

3.2.2.6. Cataclasites (C). Cataclastic marble has been subdivided in 2 categories:

(1) Corridors of breccia which are concentrated in a zone between 100 and 400 m away from the contact with the ophiolite, have preferentially developed parallel to the main foliation and dip at moderate angles toward the west north-west. Decimeter to meter thick ultracataclastic joints and microbreccias occur locally and are organized in connected branches. The brecciated zones cut across, hence mechanically rework the protolith, protomylonite and mylonite marble types (Fig. 7C). The host rock surrounding the brecciated zones experienced an intense in-situ brittle fracturing mainly characterized by millimeter scale cracks and joints (Fig. 7D). Within the brecciated corridors, we observed a gradual fragment size reduction from the fault-wall toward the central part of the deformed zones, often accompanied with a marked change in matrix color from brown to yellow. The matrix contains a high percentage of secondary phases such as quartz and dolomite (Fig. 8E). All of these features from the faulted rocks are consistent with fluid-assisted brittle mechanisms of grain size reduction.

(2) Massive tectonic breccias which are associated with steep strike-slip faults crossing the entire Kaman zone and the intrusives with a ~N070°E trend. These major dextral strike-slip faults are consistently plunging at high angles toward the south and carry a small normal component (low angle oblique slickenlines on fault planes). Megabreccias that developed only a few meters away from the fault zone contains decimeter to meter scale broken fragments, separated from each other by a fine-grained red matrix. The red color of the matrix is likely due to ferric oxi-hydroxide mineralizations by enriched fluids circulating into open faults. The presence of graded and crosscutting lamination of the fine-grained matrix in between clasts present in the fault zone suggests the activity of fluids, transport and deposition of material within fault-related voids (Fig. 7E).

3.2.2.7. Statically recrystallized marble (SR). Further east, the marble grain size increases up to centimeter-sized crystals at the vicinity of the western border of the Baranadağ intrusive and associated major dikes (up to ~300 m-wide) (Fig. 6A). Within this zone, the main foliation becomes steeper until nearly vertical. Marbles that are situated in direct contact with the intrusives are crosscut by oblique crosscutting veins (Fig. 7F). The very coarse grains of calcite are equigranular and characterized by an euhedral and polygonal shape, no undulose extinction, rare twins, and no features pointing to internal deformation. All of these microstructural properties are consistent with static recrystallisation of the marble at high temperature (Fig. 8G).

4. The contact between the Kırşehir metamorphics and the Baranadağ quartz-monzonite close to Ömerhacılı

From Kaman, the Baranadağ quartz-monzonitic pluton extends over 12 km toward the east. The eastern border of the magmatic body near the village of Ömerhacılı is characterized by an irregular contact with the metamorphic rocks. Close to Ömerhacılı, the metamorphics locally display exposures of pure marble where we carried out a detailed structural analysis (Fig. 5B). The surrounding metamorphic rocks of the area show a gradual transition to more pelitic compositions, suggesting that these rocks represent a somewhat lower part of the lithological succession. The irregular pattern of the contact between igneous and metamorphic rocks is enhanced by the presence of numerous one to 10 m scale dikes cutting at a high angle across the shallow-dipping foliated host rock. In a few cases, marble blocks have been isolated as roof pendants on top of the pluton. The monzonitic intrusion contains very coarse euhedral phenocrysts of potassic feldspar accompanied by smaller minerals of plagioclase, hornblende and quartz. These minerals do not show any trace of ductile deformation and

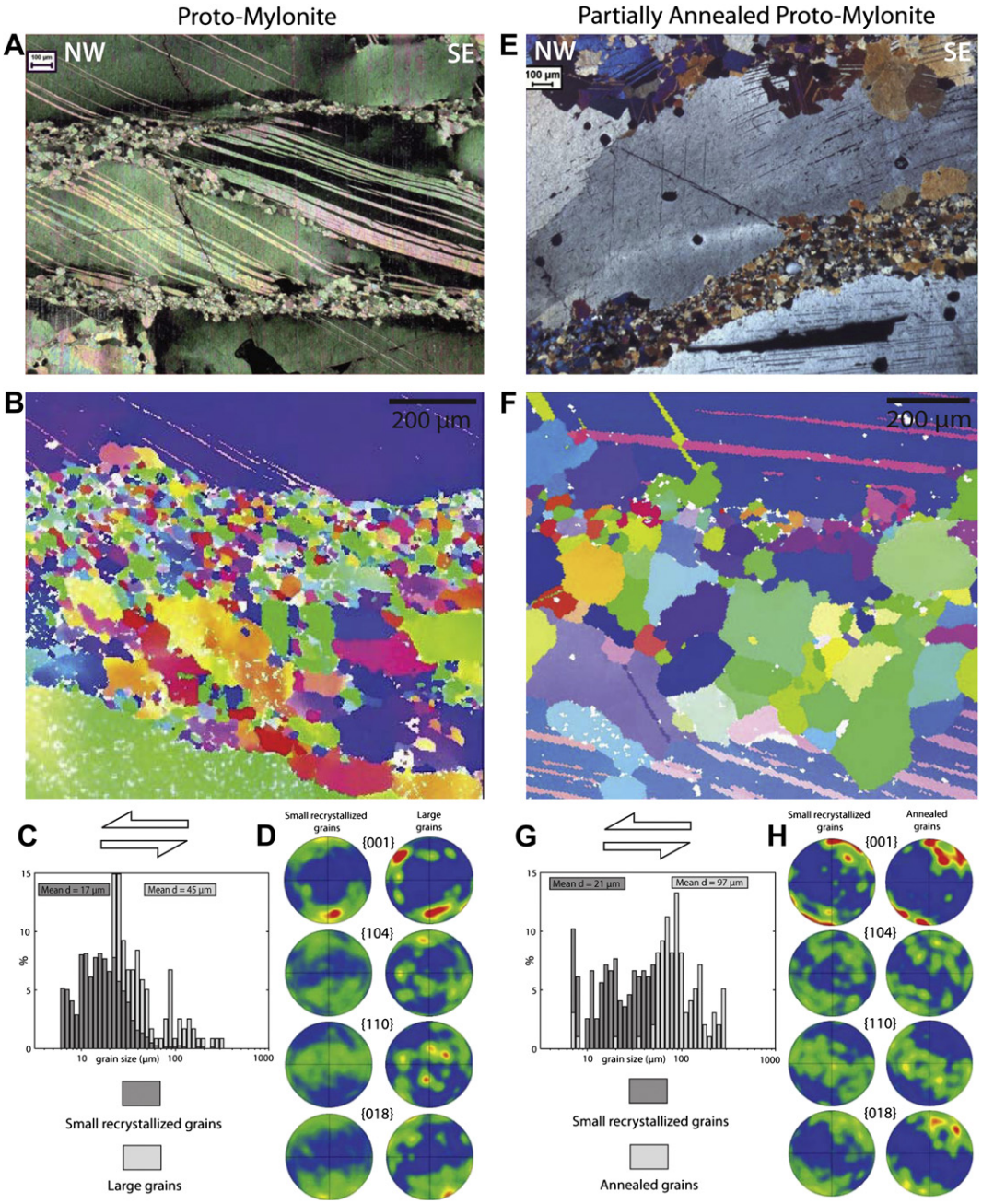

Fig. 9. A,E) Micrographs of the protomylonite and partially annealed protomylonite type fabrics at higher magnification, B,F) Orientation maps measured by EBSD, focused on the fine-grained shear bands (measurements are colour-coded by orientation). C,G) Grain size histograms from recrystallised grains in the shear bands Grain boundaries have been defined by lattice misorientations larger than 10°. D,H) Contoured c-, r-, a- and e-axes pole figures based on EBSD measurements for the small and large grains within C and D.

the entire magmatic body is generally considered as undeformed. The carbonate-rich rocks preserve a main foliation pattern, which is very similar to the one described from Kaman (average trend is N015°E, dipping 33° toward the W-NW) (Fig. 5C). Close to the dykes, we observed mega crystals of calcite with grain sizes typically in the range of centimeters. This macro-fabric is preserved in the marbles at distances of up to hundreds of meters away from the dykes and the main pluton. At about 200–400 m away from the main intrusive contact, a progressive transition occurs from complete static recrystallisation to protolithic ribboned marble. In the transition zone, discrete crosscutting protomylonitic bands have been found with peculiar coarse-grained porphyroclasts. We termed this special fabric *Partially Annealed Protomylonite* (*PA-PM*) as we can recognize an intermediate stage between protomylonitic and statically recrystallized marble (Fig. 8F). Protomylonitic features are represented by the presence of large twinned clasts with serrated grain boundaries, surrounded by interconnected bulged grains, and parallel to oblique bands of dynamically recrystallized smaller grains. The twins of the large grains are straight, slightly bend and discontinuous which make them belonging to type IV twins indicating temperatures above 250 °C (Burkhard, 1993). The static growth of these grains is identifiable from the presence of leftover small grains consumed by the larger ones, grain boundary migration over the shear bands, highly lobate grain boundaries and bulging of twin boundaries (Fig. 8F). Those features are characteristic of processes involving annealing of the protomylonite bands during high-temperature static recrystallisation.

We investigated the fine-grained fabrics within the shear bands using EBSD techniques.The shear band analyzed contains two types of recrystallized grains: 1) small equant grains with an average size of 21 μm. Those small grains have the same size and shape as the dynamically recrystallized grains from the Kaman protomylonites and we infer that they were formed during dynamic recrystallization and progressive localization of deformation; 2) larger grains (average grain size 97 μm) with very irregular lobate grain boundaries. Those grains contain very little or no internal deformation and show growth of certain grains at the expense of other grains (Fig. 9E and F). We interpret these larger grains as the result of static annealing at higher temperatures due to the intrusion of the pluton after protomylonitic deformation.

Pole figures show that the small dynamically recrystallized grains have a similar CPO as the larger annealed recrystallized grains. The typical CPO formed in the grains from the shear band is apparently retained in the newly grown annealed grains. It follows that annealing did not obliterate the previously formed deformation-related CPO, which is in good agreement with similar results from experimental annealing studies (Barnhoorn et al., 2005) (Fig. 9H).

The orientations of shear zones, mineral lineations and associated senses of shear for the Ömerhacılı area are summarized in Fig. 5. The inferred shearing orientation and kinematics on shear bands show a pattern, which is nearly identical to that in Kaman, with a consistent top-to-WNW shear motion.

5. Synthesis - discussion

5.1. The first extensional detachment described from the northern CACC

The carbonate-rich metasediments exposed around Kaman belong to the upper part of the metamorphosed lithology. The nature of the deformation of these metamorphic rocks in the vicinity of the ophiolite-derived materials places constrains on the nature of the contact. The mineral assemblages from the essentially unmetamorphosed ophiolitic hanging wall and the high-grade marble-rich footwall indicate a major metamorphic gap across the contact. In terms of deformation, the hanging wall is affected by conjugate semi-brittle normal faults.

In the footwall, five distinctive marble type fabrics have been identified. The coarse-grained protolith type associated with the main metamorphic foliation is crosscut by discrete protomylonitic and mylonitic shear bands. Shear sense indicators such as asymmetric calcite σ-clasts, consistent sets of oblique twins in calcite porphyroclacts and dynamically recrystallized grain shape preferred orientations all indicate top-to-W-NW normal shearing. Toward the contact, the ductile structures have been overprinted by brittle structures and reworked into localized cataclastic breccia zones developed in the same low angle orientation below the ophiolite. Therefore, the structural evolution recorded in the marbles and presented in the cross section of Fig. 5 suggests a continuous deformation history from ductile to brittle conditions during cooling and exhumation and is clearly consistent with the typical evolution described from extensional detachment zones (Lister and Davis, 1989).

In addition, the spatial distribution and evolution of the calcite fabrics in the Kaman area is very similar to that described from the shear zone complex on Thassos Island in Greece, associated with a major crustal-scale extensional detachment, and also developed in a marble-dominated lithology (Bestmann et al., 2000).

We note that the term Kırşehir Metamorphic Core Complex (KMCC) has already been proposed in the literature (Genç, 2004), but referring to an inferred post Middle-Eocene detachment fault in the vicinity of Savcılı village. However, the nature of this structure is currently debated, as other authors argue for a thrust contact (Seymen, 2000; Isik et al., 2010).

5.2. Stages of deformation, and the rate and timing of exhumation in Kaman

Our structural analysis on marble fabrics provides important constraints on the successive events that affected the Kaman-Ömerhacılı area. We supplement these results with published geochronological data to construct Pressure-time and Temperature-time trajectories for the Kırşehir metamorphics from their regional metamorphism to their final unroofing. In order to summarize this information in a simple way, we propose a conceptual geotectonic model in four stages illustrating the main evolution of the metamorphic rocks and their exhumation (Fig. 10A and B).

5.2.1. Stage 1: Alpine regional metamorphism

From the Kaman zone, constraints on peak metamorphic conditions are pressure-temperature estimates on high-grade garnet-sillimanite metapelites giving ~700–750 °C for 6–7 kbar, and a growth age of monazite of 84.1 ± 0.8 Ma (U/Pb SHRIMP analysis) (Whitney et al., 2001; Whitney and Hamilton, 2004). Therefore, during Santonian times the Kaman zone was buried at ~20 km depth and underwent clearly high temperature metamorphic conditions. During this regional high temperature event, deformation led to the development of the main syn-metamorphic foliation, and associated isoclinal folds. We ascribe the protolith-type marble and its highly twinned, coarse equigranular calcite microstructure to this regional high temperature stage.

5.2.2. Stage 2: fast exhumation accompanied with ductile shearing

Following peak metamorphism, the metamorphic sequence rose up through the crust to relatively shallow levels where it became intruded by large plutons. Titanite and zircon crystallization ages on the neighboring quartz-monzonites are ~74 Ma, and intrusion occurred at relatively shallow crustal levels (10–12 km depth) (Köksal et al., 2004; Boztuğ et al., 2009a). Age and depth of both metamorphism and magmatism indicate that the Kaman zone traveled some 10 km vertically through the crust in a time span of 10 Ma, which corresponds to a fast rate of exhumation during the early Campanian (~1 km/Ma). In the case of the Kaman area, we suggest that this stage of fast exhumation was accommodated, in the upper crust, by ductile shear zones cutting through the metamorphic foliation. These shear bands indicate ongoing localization of the deformation, leading to a microstructure of internally deformed coarse-grained clasts and very fine dynamically recrystallized grains. The absence of dolomite in the protomylonite type marble has unfortunately precluded in-situ thermometry (Mg equilibrium between calcite and dolomite) to estimate the ambient temperature range during the formation of the protomylonitic fabric. However, by comparison with very similar microstructures from the Thassos Island shear zone (Bestmann et al., 2000; Bestmann and Prior, 2003), and combined with the published recrystallized grain size/temperature dependence trend in naturally deformed calcite rocks (De Bresser et al., 2002), it seems reasonable to estimate the metamorphic temperature during the development of the protomylonitic shear bands (with an average size of dynamically recrystallized grains of ~20 μm) in Kaman around 300–400 °C.

5.2.3. Stage 3: magmatic intrusion at shallow crustal levels

In addition to the clearly crosscutting relationships between the metamorphic rocks and the magmatic plutons and dikes in the field, microstructural evidence strongly suggests static overgrowth

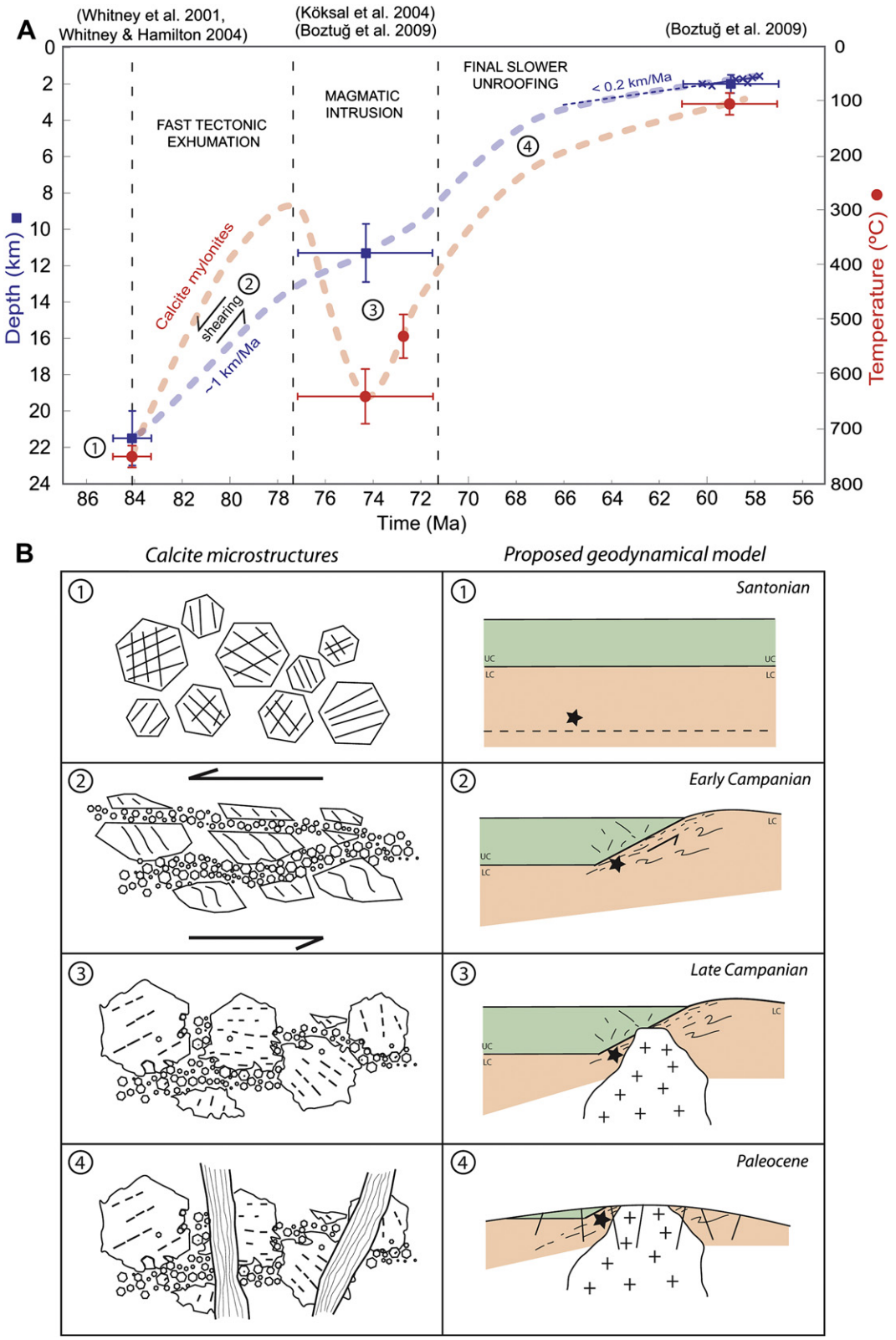

Fig. 10. A) Pressure/time and Temperature/time trajectories for the Kaman metamorphics based on present microstructural evidence and geochronological data from the literature. B) Conceptual tectonic model in 4 stages illustrating the tectonometamorphic evolution of the Kaman-Ömerhacılı rocks during their exhumation. For each stage, typical calcite microstructures as observed in the field are linked to the model.

(annealing) of the protomylonitic microstructure in the Ömerhacılı area. The only appreciable explanation for this post-deformational annealing is local heating in the vicinity of the intruding pluton. Al/Ti thermometers on amphiboles indicate a temperature of crystallization of the monzonite at 600–750 °C (Ilbeyli, 2005; Boztuğ et al., 2009a). This demonstrates that the intrusion reheated a relatively cooled metamorphic sequence during late Campanian times. Consistent with this idea, (Genç, 2004) has noted that the hosted migmatite dome close to Savcılı displays discordant, sub-vertical and east-west trending gold-bearing quartz veins formed during magmatism and suggesting release of metamorphic fluids from depth while the metamorphic rocks already arrived at shallow crustal levels. Intrusion of the Baranadağ quartz-monzonite post-dated ductile deformation, as it displays intrusive rather than tectonic contacts with the metamorphic host rocks, and shows no evidence for ductile fabrics itself. On both sides of the magmatic body, there is no significant change in main direction of foliation planes and associated crosscutting sets of shear zones. Therefore, we interpret that the original geometry of the pre-intrusion deformation zone remained unchanged during the magmatic event.

At the scale of the CACC, it is generally accepted that the CAM and the ophiolites (CAO) were both intruded by mostly undeformed intrusives (Erler and Göncüoğlu, 1996). Therefore, and in view of the crosscutting and static heating relationships between the metamorphic and magmatic rocks; we suggest that the accommodation of the ductile deformation via detachment faults located at the boundary between the metamorphics and the ophiolites such as described in Kaman, ceased at this time. A similar scenario has already been proposed for the Mojave Desert (California), where the cessation of active extensional detachment zone has been ascribed to intrusion of a high-level pluton across it (Davis et al., 1993). Any ongoing extensional denudation must have occurred by brittle faulting.

5.2.4. Stage 4: final exhumation at slower rate

After intrusion, the metamorphic/igneous complex behaved as one single crustal unit. $^{40}Ar/^{39}Ar$ dating of amphiboles from the Baranadağ quartz-monzonite yielded cooling ages of 69–72 Ma (cooling below ~500 °C) and apatite fission-track analysis gave ages around 57–60 Ma (Boztuğ and Jonckheere, 2007; Boztuğ et al., 2009a). Based on the apatite fission-track data, a rapid exhumation rate (>1 km/Ma) has been estimated for all of the Camsarı, Hamit, Durmuşlu and Baranadağ plutons (Boztuğ et al., 2009a). However, the apatite fission-track age versus elevation plot from the Baranadağ quartz-monzonite itself, rather suggests a slower exhumation rate below 0.2 km/Ma (Fig. 10A).

The intrusive body is not ductily deformed, but was affected by brittle deformation after its emplacement, as faults displace the boundaries of the pluton. This brittle phase led to a well-developed network of N070°E trending steep dextral strike-slip faults with a small normal component, cutting across both the metamorphic rocks and the monzonites. We tend to conclude that the later stages of exhumation in the Kaman and Ömerhacılı areas proceeded at a slower rate that previously considered, and that this part of the exhumation history was accomodated by brittle tectonics coupled with erosion until reaching the surface in Late Paleocene (Kaymakci et al., 2009).

5.3. Role of tectonics during exhumation at the scale of the CACC

The presence of an extensional detachment below the ophiolitic unit in the Kaman region is a newly recognized feature and supports the role of tectonics during the exhumation of the Kırşehir massif. However, the presence of domains of massive marbles intruded by the Çelebi granitoids west of Kaman indicates that the inferred structure might not be the original place where the detachment rooted in the middle or lower crust. We may consider that the main extensional zone is located in the west (30–40 km away) and that the Kaman zone represents the prolongation of a large-scale flat-lying detachment zone. However, our structural data in Kaman do not provide any evidence for the activity of the fault zone under amphibolite conditions, as the inferred marble ductile shear bands indicate deformation at upper crustal levels. A possible alternative interpretation would be that the contact close to Kaman is a secondary or coeval imbricated inner detachment within a larger extensional setting, such as described from the Menderes massif (Bozkurt and Oberhansli, 2001; Ring et al., 2003, van Hinsbergen, 2010).

At the scale of the Kırşehir massif, large exposures of volcanic rocks represent the cogenetic extrusives related to the central Anatolian intrusives. These volcanic rocks rest directly on top of the metamorphics with a faulted contact (for example close to Sorgun, Fig. 3), which indicates that tectonics must be responsible for a significant part of the final exhumation of the Kırşehir metamorphic rocks to the surface.

At the scale of the CACC, other extensional features have already been previously described. In the Niğde massif, rocks from the lower metamorphic unit record top-to-the-NE/ENE shearing along the contact with ophiolitic gabbros (Gautier et al., 2002), and discrete ductile extensional shear zones cutting through the Yozgat and Ağaçören batholiths respectively record top-to NW and top-to SW motions, dated around 72 Ma (Isik et al., 2008; Isik, 2009).

Our results support Gautier et al. (2002) suggestion that a synchronous high-magnitude extension may have occurred at the scale of the CACC during the late Cretaceous. However, the regional east-west direction of extension during exhumation (Gautier et al., 2008) is difficult to explain in its present configuration, as shearing motions show no clear consistency at the larger scale.

In order to completely evaluate the kinematics of exhumation-related shearing in the CACC, future work would be necessary on tectonic structures potentially present at the edges of the Akdağ massif.

Finally, structural and metamorphic studies carried out in the southern Niğde massif have documented that the lower unit of metasediments is associated with the highest grade of metamorphism while the upper unit mostly recorded lower grade conditions (Whitney and Dilek, 1998). In contrast, the upper unit of the metasedimentary pile near Kaman also shows the highest grade of metamorphism. It seems, therefore at the scale of the CACC, that there is no systematic relationship between the position in the metamorphic unit and the metamorphic grade.

6. Conclusions

In the area around Kaman and Ömerhacılı, high-grade metamorphic rocks of the Kırşehir massif are exposed underneath virtually non-metamorphic ophiolites, close to the Baranadağ pluton. Field- and microscale structures from the marble-rich footwall sequence indicates that the contact with the overlying ophiolites represents an extensional detachment zone. Kinematic indicators from protomylonitic shear bands point to a top-to-the-W-NW motion.

The tectonometamorphic evolution of the area, from regional Alpine peak metamorphism to final unroofing at the Earth's surface, involved two different stages of exhumation.

(1) The metamorphic rocks underwent localized ductile shearing between 20 and 10 km depth involving an upper-crustal extensional detachment zone, leading to fast exhumation at a rate of ~1 km/Ma. This occurred between peak metamorphism (~84 Ma) and shallow crustal intrusion of the Baranadağ pluton (~74 Ma). Prior to intrusion, the metamorphic sequence cooled

down to 300–400 °C in Late Campanian times. (2) The second and final phase of exhumation, bringing the metamorphic/igneous complex to the surface during the Paleocene, occurred at a much slower rate, and was accommodated by brittle upper crustal tectonics coupled with erosion processes.

In combination with the existing data, the Kaman structures demonstrate that tectonics did play an important role in the regional-scale exhumation of metamorphic rocks in the CACC. The newly recognized extensional detachment in the northern Kırşehir massif may be part of a larger scale system, which may have rooted further west.

Acknowledgments

We thank Steve Smith and Uwe Ring for critical reviews of our manuscript. This work was financially supported by the Netherlands Research Centre for Integrated Solid Earth Sciences (ISES), the Netherlands Organisation for Scientific Research (NWO) and the DARIUS Programme.

References

Akiman, O., Erler, A., Göncüoğlu, M.C., Güleç, N., Geven, A., Türeli, T.K., Kadioğlu, Y.K., 1993. Geochemical characteristics of granitoids along the western margin of the CACC and their tectonic implications. Geological Journal 28, 371–382.

Aydin, S.N., Önen, A.P., 1999. Field, petrographic and geochemical features of the Baranadağ quartz monzonite of the Central Anatolian granitoids, Turkey. Turkish Journal of Earth Sciences 8, 113–123.

Aydin, S.N., Göncüoğlu, M.C., Erler, A., 1998. Latest Cretaceous magmatism in the CACC: review of field, petrographic and geochemical features. Turkish Journal of Earth Sciences 7, 259–268.

Bailey, E., McCallien, W.J., 1950. The Ankara Melange and the Anatolian thrust. Bulletin of the Mineral Research and Exploration Institute of Turkey 40, 12–22.

Barnhoorn, A., Bystricky, M., Burlini, L., Kunze, K., 2005. Post-deformational annealing of calcite rocks. Tectonophysics 403 (1–4), 167–191.

Bestmann, M., Prior, D.J., 2003. Intragranular dynamic recrystallization in naturally deformed calcite marble: diffusion accommodated grain boundary sliding as a result of subgrain rotation recrystallization. Journal of Structural Geology 25 (10), 1597–1613.

Bestmann, M., Kunze, K., Matthews, A., 2000. Evolution of a calcite marble shear zone complex on Thassos Island, Greece: microstructural and textural fabrics and their kinematic significance. Journal of Structural Geology 22 (11–12), 1789–1807.

Bozkurt, E., Oberhansli, R., 2001. Menderes Massif (western Turkey): structural, metamorphic and magmatic evolution - a synthesis. International Journal of Earth Sciences 89 (4), 679–708.

Boztuğ, D., Güney, O., Heizler, M., Jonckheere, R.C., Tichornirowa, M., Otlu, N., 2009a. 207 Pb-206 Pb, 40 Ar-39 Ar and fission-track geothermochronology quantifying cooling and exhumation history of the Kaman-Kırşehir region intrusions, central Anatolia, Turkey. Turkish Journal of Earth Sciences 18, 85–108.

Boztuğ, D., Jonckheere, R.C., 2007. Apatite fission track data from central Anatolian granitoids (Turkey). Constraints on Neo-Tethyan Closure. Tectonics 26 (3).

Boztuğ, D., Jonckheere, R.C., Heizler, M., Ratschbacher, L., Harlavan, Y., Tichomirova, M., 2009b. Timing of post-obduction granitoids from intrusion through cooling to exhumation in central Anatolia, Turkey. Tectonophysics 473 (1–2), 223–233.

Boztuğ, D., Tichomirowa, M., Bombach, K., 2007. 207Pb-206Pb single-zircon evaporation ages of some granitoid rocks reveal continent-oceanic island arc collision during the Cretaceous geodynamic evolution of the central Anatolia, Turkey. Journal of Asian Earth Sciences 31, 71–86.

Burkhard, M., 1993. Calcite twins, their geometry, appearance and significance as stress-strain markers and indicators of tectonic regime: a review. Journal of Structural Geology 15 (3–5), 351–368.

Çemen, I., Göncüoğlu, M.C., Dirik, K., 1999. Structural evolution of the Tuzgölü basin in central Anatolia, Turkey. Journal of Geology 107 (6), 693–706.

Candan, O., Cetinkaplan, M., Oberhansli, R., Rimmele, G., Akal, C., 2005. Alpine high-pressure low-temperature metamorphism of the Afyon zone and implications for the metamorphic evolution of western Anatolia, Turkey. Lithos 84 (1–2), 102–124.

Davis, G.A., Fowler, T.K., Bishop, K.M., Brudos, T.C., Friedmann, S.J., Burbank, D.W., Parke, M.A., Burchfiel, B.C., 1993. Pluton Pinning of an active Miocene detachment fault system, eastern Mojave desert, California. Geology 21 (7), 627–630.

De Bresser, J.H.P., Evans, B., Renner, J., 2002. On Estimating the Strength of Calcite Rocks Under Natural Conditions. In: Geological Society of London, Special Publications 200, pp. 309–329.

Dirik, K., Göncüoğlu, M.C., Kozlu, H., 1999. Stratigraphy and pre-miocene tectonic evolution of the SW part of the Sivas basin, central Anatolia, Turkey. Geological Journal 34, 303–319.

Erdoğan, B., Akay, E., Uğur, M.S., 1996. Geology of the Yozgat region and evolution of the collisional Çankırı basin. International Geology Review 38, 788–806.

Erkan, E., 1976. Isogrades determined in the regional metamorphic area surrounding Kırşehir and their petrological interpretation. Yerbilimleri 2 (1), 23–54 (in Turkish with English summary).

Erler, A., Göncüoğlu, M.C., 1996. Geologic and tectonic setting of the Yozgat Batolith, northern central Anatolian crystalline complex, Turkey. International Geology Review 38, 714–726.

Fayon, A.K., Whitney, D.L., Teyssier, C., Garver, J.I., Dilek, Y., 2001. Effects of plate convergence obliquity on timing and mechanisms of exhumation of a mid-crustal terrain, the central Anatolian crystalline complex. Earth and Planetary Science Letters 192 (2), 191–205.

Floyd, P.A., Göncüoğlu, M.C., Winchester, J.A., Yaliniz, M.K., 2000. In: Geochemical Character and Tectonic Environment of Neotethyan Ophiolitic Fragments and Metabasites in the Central Anatolian Crystalline Complex, Turkey. Geological Society Special Publication 173, pp. 183–202.

Göncüoğlu, M.C., 1977. Geologie des westlichen Niğde Massivs. Phd Thesis, Bonn University.

Göncüoğlu, M.C., 1986. Geochronological data from the southern part (Niğde area) of the Central Anatolian Massif. Bulletin of the Mineral Research and Exploration Institute of Turkey 105–106, 83–96.

Göncüoğlu, M.C., 1992. Structural and stratigraphic framework of the central anatolian tertiary basins. Introduction to the Early Paleogene of the Haymana-Polatlı basin, Field-trip book IGCP Project N.286 Early Paleogene Benthos Third Meeting, Ankara (Turkey)(October 08–13).

Göncüoğlu, M.C., Erler, A., Toprak, V., Yaliniz, K.M., Olgun, E., Rojay, B., 1992. Geology of the Western Part of the Central Anatolian Massif, Part 2: Central Section. Turkish Petroleum Corporation (TPAO), Report no. 3155, 76 pp (in Turkish).

Göncüoğlu, M.C., Toprak, V., Kuşcu, I., Erler, A., Olgun, E., 1991. Geology of the Western Part of the Central Anatolian Massif, Part 1: Southern Section. Turkish Petroleum Corporation (TPAO), Report no. 2909, 140 pp (in Turkish).

Görür, N., Oktay, F.Y., Seymen, I., Şengör, A.M.C., 1984. Palaeotectonic Evolution of the Tuzgölü Basin Complex, Central Turkey: Sedimentary Record of a Neo-Tethyan Closure. In: Geological Society, London, Special Publications 17, 1 467–482.

Görür, N., Tüysüz, O., Şengör, A.M.C., 1998. Tectonic evolution of the central Anatolian basins. International Geology Review 40 (9), 831–850.

Gautier, P., Bozkurt, E., Hallot, E., Dirik, K., 2002. Dating the exhumation of a metamorphic dome: geological evidence for pre-eocene unroofing of the Niğde Massif (central Anatolia, Turkey). Geological Magazine 139 (5), 559–576.

Gautier, P., Bozkurt, E., Bosse, V., Hallot, E., Dirik, K., 2008. Coeval extensional shearing and lateral underflow during Late Cretaceous core complex development in the Niğde Massif, Central Anatolia, Turkey. Tectonics 27 (1).

Genç, Y., 2004. Savcılı migmatite-dome hosted gold-quartz veins in Kırşehir Metamorphic Core Complex (KMCC), Central Anatolia, Turkey. Proceedings of the 5th International Symposium on Eastern Mediterranean Geology, Thessalloniki, Greece, April 2004, vol. 3, (1394-1397), pp. 14–20.

Ilbeyli, N., 2005. Mineralogical-geochemical constraints on intrusives in central Anatolia, tectono-magmatic evolution and characteristics of mantle source. Geological Magazine 142 (2), 187–207.

Ilbeyli, N., Pearce, J.A., Thirlwall, M.F., Mitchell, J.G., 2004. Petrogenesis of Collision-related Plutonics in Central Anatolia, vol. 72. Lithos, Turkey, pp. 163–182.

Isik, V., 2009. The ductile shear zone in granitoid of the central anatolian crystalline complex, Turkey: implications for the origins of the Tuzgölü basin during the late Cretaceous extensional deformation. Journal of Asian Earth Sciences 34 (4), 507–521.

Isik, V., Lo, C.-H., Göncüoğlu, C., Demirel, S., 2008. 39Ar/40Ar ages from the Yozgat batholith: preliminary data on the timing of late Cretaceous extension in the central anatolian crystalline complex, Turkey. The Journal of Geology 116 (5), 510–526.

Isik, V., Seyitoglu, G., Caglayan, A., Uysal, T., Zhao, J., Sozeri, K., Esat, K., 2010. Cataclastic Zones within the Savcılı Fault Zone, Central Turkey. American Geophysical Union Fall Meeting 2010 (abstract #T51A-2011).

Jolivet, L., Faccenna, C., Goffe, B., Burov, E., Agard, P., 2003. Subduction tectonics and exhumation of high-pressure metamorphic rocks in the mediterranean orogens. American Journal of Science 303 (5), 353–409.

Jolivet, L., Lecomte, E., Huet, B., Denele, Y., Lacombe, O., Labrousse, L., Le Pourhiet, L., Mehl, C., 2010. The north cycladic detachment system. Earth and Planetary Science Letters 289 (1–2), 87–104.

Köksal, S., Göncüoğlu, M.C., Floyd, P.A., 2001. Extrusive members of postcollisional A-type magmatism in central Anatolia: karahidir volcanics, Idiş Dağı - Avanos area, Turkey. International Geology Review 43 (8), 683–694.

Köksal, S., Romer, R.L., Göncüoğlu, M.C., Toksoy-Köksal, F., 2004. Timing of post-collisional H-type to A-type granitic magmatism: U-Pb titanite ages from the alpine central Anatolian granitoids (Turkey). Inernational Journal of Earth Sciences 93, 974–989.

Kadıoğlu, Y.K., Dilek, Y., Foland, K.A., 2006. Slab Break-off and Syncollisional Origin of the Late Cretaceous Magmatism in the Central Anatolian Crystalline Complex, Turkey. In: Geological Society of America Special Papers 409, pp. 381–415.

Kaymakci, N., Özçelik, Y., White, S.H., Van Dijk, P.M., 2009. Tectono-stratigraphy of the Çankırı Basin: Late Cretaceous to Early Miocene Evolution of the Neotethyan Suture Zone in Turkey. In: Geological Society, London, Special Publications 311, 1 67–106.

Kocak, K., Leake, B.E., 1994. The petrology of the Ortakoy district and its ophiolite at the western edge of the middle Anatolian Massif, Turkey. Journal of African Earth Sciences 18 (2), 163–174.

Lister, G.S., 1984. Metamorphic core complexes of cordilleran type in the cyclades, Aegean Sea, Greece. Geology 12 (4), 221–225.

Lister, G.S., Davis, G.A., 1989. The origin of metamorphic core complexes and detachment faults formed during tertiary continental extension in the northern Colorado river region, USA. Journal of Structural Geology 11 (1–2), 65–94.
Okay, A.I., Tüysüz, O., 1999. Tethyan sutures of northern Turkey. In: Durand, B., Jolivet, L., Horváth, F., Séranne, M. (Eds.), The Mediterranean Basins: Tertiary Extension Within the Alpine Orogen. Geological Society, London, Special Publications 156, pp. 475–515.
Okay, A.I., Harris, N.B.W., Kelley, S.P., 1998. Exhumation of blueschists along a Tethyan suture in northwest Turkey. Tectonophysics 285 (3–4), 275–299.
Otlu, N., Boztuğ, A., 1998. The coexistence of the silica oversaturated (ALKOS) and undersaturated alkaline (ALKUS) rocks in the Kortundağ and Baranadağ plutons from the central Anatolian alkaline Plutonism, east Kaman / NW Kırşehir, Turkey. Turkish Journal of Earth Sciences 7, 241–257.
Pourteau, A., Candan, O., Oberhänsli, R., 2010. High-pressure metasediments in central Turkey: constraints on the Neotethyan closure history. Tectonics 29 (5), TC5004.
Ring, U., Johnson, C., Hetzel, R., Gessner, K., 2003. Tectonic denudation of a Late Cretaceous-Tertiary collisional belt: regionally symmetric cooling patterns and their relation to extensional faults in the Anatolide belt of western Turkey. Geological Magazine 140 (4), 421–441.
Ring, U., Will, T., Glodny, J., Kumerics, C., Gessner, K., Thomson, S., Gungor, T., Monie, P., Okrusch, M., Druppel, K., 2007. Early exhumation of high-pressure rocks in extrusion wedges: Cycladic blueschist unit in the eastern Aegean, Greece, and Turkey. Tectonics 26 (2).
Ring, U., Glodny, J., Will, T., Thomson, S., 2010. The Hellenic subduction system: high-pressure metamorphism, exhumation, normal faulting, and large-scale extension. Annual Review of Earth and Planetary Sciences vol. 38 (38), 45–76.
Şengör, A.M.C., Yilmaz, Y., 1981. Tethyan evolution of Turkey: a plate tectonic approach. Tectonophysics 75 (3–4), 181–241.
Seymen, I., 1981. Stratigraphy and metamorphism of the Kırşehir Massif around Kaman (Kırşehir - Turkey). Bulletin of Geological Society of Turkey 24, 7–14.
Seymen, I., 1982. Kaman Dolayında Kırşehir masifi'nin Jeolojisi. ITÜ Maden Fakültesi, Doçentlik Tezi, Istanbul, p. 164.
Seymen, I., 1983. Tectonic features of Kaman group in comparison with those of its neighbouring formations around Tamadağ (Kaman-Kırşehir). Bulletin of Geological Society of Turkey 26, 89–98.
Seymen, I., 1984. Geological evolution of the metamorphic rocks in the Kırşehir Massif. Ketin Simpozyumu, 133–148.
Seymen, I., 2000. Geology of the Kırşehir Massif between the Savcılıbeyit (Kaman) and Yeşilli (Kırşehir) villages. Congress of Geosciences and Mining for the 75th Anniversary of the Turkish Republic. Proceedings Book 1, MTA Ankara, 67–91 (in Turkish with english abstract).
Tüysüz, O., Dellaloglu, A.A., Terzioglu, N., 1995. A magmatic belt within the neotethyan suture zone and its role in the tectonic evolution of northern Turkey. Tectonophysics 243 (1–2), 173–191.
Tolluoğlu, A.Ü, Erkan, Y., 1989. Regional progressive metamorphism in the central Anatolian crystalline basement, NW Kırşehir Massif, Turkey. METU Journal of Pure and Applied Sciences 22 (3), 19–41.
Teklehaimanot, L.T., 1993. Geology and Petrography of Gülşehir area, Nevşehir, Turkey. MSc thesis, Middle East Technical University, Ankara, Turkey, [unpublished].
Umhoefer, P.J., Whitney, D.L., Teyssier, C., Fayon, A.K., Casale, G., Heizler, M.T., 2007. Yo-yo Tectonics in a Wrench Zone, Central Anatolian Fault Zone, Turkey. In: Geological Society of America Special Papers 434, pp. 35–57.
Vache, R., 1963. Akdağmadeni kontak yatakları ve bunların Orta Anadolu Kristalinine karşı olan jeolojik çerçevesi. Bulletin of the Mineral Research and Exploration Institute of Turkey 60, 20–34 (in Turkish with English Abstract).
van Hinsbergen, D.J.J., 2010. A key extensional metamorphic complex reviewed and restored: the Menderes Massif of western Turkey. Earth-Science Reviews 102 (1–2), 60–76.
Whitney, D.L., Dilek, Y., 1998. Metamorphism during alpine crustal thickening and extension in central Anatolia, Turkey: the Niğde metamorphic core complex. Journal of Petrology 39 (7), 1385–1403.
Whitney, D.L., Hamilton, M.A., 2004. Timing of high-grade metamorphism in central Turkey and the assembly of Anatolia. Journal of the Geological Society 161, 823–828.
Whitney, D.L., Teyssier, C., Dilek, Y., Fayon, A.K., 2001. Metamorphism of the central Anatolian crystalline complex, Turkey: influence of orogen-normal collision vs, wrench-dominated tectonics on P-T-t paths. Journal of Metamorphic Geology 19 (4), 411–432.
Whitney, D.L., Teyssier, C., Fayon, A.K., Hamilton, M.A., Heizler, M., 2003. Tectonic controls on metamorphism, partial melting, and intrusion: timing and duration of regional metamorphism and magmatism in the Niğde Massif, Turkey. Tectonophysics 376 (1–2), 37–60.
Yaliniz, K.M., Göncüoğlu, M.C., 1998. General geological characteristics and distribution of the central Anatolian ophiolites. Yerbilimleri 20, 19–30.
Yaliniz, M.K., Göncüoğlu, M.C., Ozkan-Altiner, S., 2000. Formation and emplacement ages of the SSZ-type neotethyan ophiolites in central Anatolia, Turkey: palaeotectonic implications. Geological Journal 35 (2), 53–68.